

## Ghrelin alleviates hypoxia/reoxygenation-induced H9C2 injury by activating autophagy and AMPK/ULK1 pathway

Hui Liu<sup>1</sup>, Wei Lv<sup>2</sup>, Li Ouyang<sup>3</sup>, Li Xu<sup>4\*</sup><sup>1</sup>Department of Thyroid Surgery, Jinan Central Hospital, Jinan 250013, China<sup>2</sup>Department of Cardiovascular Unit2, Jinan Central Hospital, Jinan 250013, China<sup>3</sup>Department of Surgery, Outpatient Department of 94201 PLA, Jinan 250013, China<sup>4</sup>Department of Cardiology Intensive Care, Central Hospital Affiliated to ShanDong First Medical University, Jinan 250013, China

### ARTICLE INFO

#### Original paper

#### Article history:

Received: September 08, 2023

Accepted: November 09, 2023

Published: November 15, 2023

#### Keywords:

*Ghrelin, hypoxia/reoxygenation, inflammatory, autophagy, AMPK/ULK1 pathway*

### ABSTRACT

The research aims to explore the protective effects of ghrelin and its underlying molecular mechanisms in an H9C2 hypoxia/reoxygenation model. H9C2 cells were transfected with ghrelin overexpression lentiviral vector. The hypoxia/reoxygenation H9C2 model was constructed. The expression of ghrelin was analyzed by qRT-PCR and Western Blotting. CCK8, flow cytometry and TUNEL assay were used to analyze the impact of ghrelin on the survival and apoptosis of H9C2 injured by hypoxia/reoxygenation. The levels of autophagy-related proteins in H9C2 cells were evaluated through Western blotting. ELISA was utilized to assess how ghrelin affects the inflammatory response triggered by hypoxia/reoxygenation. Western blotting was utilized to investigate the regulatory role of ghrelin on the AMPK/ULK1 pathway. Additionally, the AMPK inhibitor Compound C was introduced to delve further into the associated mechanism. Hypoxia/reoxygenation injury decreased the expression of ghrelin. Transfection of ghrelin overexpression lentiviral vector significantly increased the expression of ghrelin in H9C2 cells. Ghrelin overexpression can significantly promote cell survival, reduce apoptosis, activate AMPK, ULK1 and AMBRA1, promote autophagy, increase the expression of LC3BII/LC3BI and Beclin-1, reduce the expression of P62, and reduce inflammatory response. Ghrelin inhibited apoptosis of H9C2 caused by hypoxia/reoxygenation and reduced inflammatory response, which mechanism is related to activation of AMPK/ULK1 pathway and autophagy.

Doi: <http://dx.doi.org/10.14715/cmb/2023.69.11.36>Copyright: © 2023 by the C.M.B. Association. All rights reserved. 

### Introduction

Ghrelin is a peptide and hormone composed of 28 amino acids (1). It is an endogenous ligand of the growth hormone secretory hormone receptor, which can regulate energy balance and body weight balance (2,3). Recent research has provided substantial evidence that the cardiovascular system is a primary target of ghrelin (4). Ghrelin has a variety of cardiovascular effects, including myocardial contractility enhancement, vascular endothelial protection and improvement of myocardial energy metabolism (5). Previous studies have shown that the effects of ghrelin in the cardiovascular system may be related to its anti-inflammatory, antioxidant, anti-myocardial and endothelial cell apoptosis (6, 7). However, the cellular and molecular mechanisms of ghrelin induced by hypoxia/reoxygenation are still unclear.

A large number of evidences show that oxidative stress and inflammation promote apoptosis, and are related to apoptosis. Apoptosis of cardiomyocytes is related to cardiovascular disease (8). Hence, it holds immense importance to investigate the molecular mechanisms underlying cardiomyocyte survival and apoptosis (9) Autophagy is a self-digestive process in which protein aggregates, impaired organelles, and lipid droplets are segregated into autophagosomes (10, 11). The fusion of autophagosome and lysosome results in the degradation of its contents (12). Mi-

cro-tubule-associated protein 1 light chain 3 (LC3) serves as a crucial regulator of autophagy (13). LC3 governs key phases of the autophagy process, including the initiation of autophagosome formation, the identification of autophagic cargo, and the fusion of autophagosomes with lysosomes (14-16). The conversion of LC3BI to LC3BII through proteolysis and lipidation is a recognized indicator of mammalian autophagy (14-16). Another sign of autophagy is the presence of dead body 1 (P62), which is subjected to degradation through the autophagic process (17).

Amp-activated protein kinase (AMPK) serves as a crucial metabolic energy sensor found in eukaryotic organisms (18). It regulates cell metabolism and maintains energy homeostasis by measuring the intracellular ratio of AMP to ATP. UC-51 like autophagy activating kinase 1 (ULK1) is a serine/threonine kinase present in mammals (19, 20). Functioning as a pivotal component of the autophagy initiation complex, ULK1 is capable of orchestrating classical autophagy processes (21). The classical autophagy reaction refers to the autophagy lysosomal pathway mediated by a series of autophagy-related proteins, which encapsulates abandoned or damaged proteins and organelles in autophagy, and then combines with lysosomes to degrade proteins and organelles in lysosomes (22, 23). Previous reports have shown that AMPK is a ULK1 interacting protein. AMPK has the capacity to phosphorylate ULK1 at a minimum of three distinct sites, and the activa-

\* Corresponding author. Email: [xl15315316725@126.com](mailto:xl15315316725@126.com)

tion of AMPK can bind to regulatory proteins and enhance the expression of ULK1-related proteins (24).

In this study, H9C2 cell apoptosis was induced by hypoxia/reoxygenation (H/R). Here, we examined whether ghrelin could activate the AMPK/ULK1 pathway and enhance autophagy.

## Materials and Methods

### Cell culture

We purchased the H9C2 cells from Beijing Beina Chuan-glian Biotechnology Research Institute (BNCC295075) and cultured them in DMEM (Cat#31600, Solarbio, Beijing, China) + 10% FBS (Cat#S9030, Solarbio, Beijing, China) + 100 U/ml penicillin and 100 U/ml streptomycin medium at 37°C.

### Cell transfection

The day prior to transfection, the cells were subjected to subculturing and cultivated within a 6-well plate to facilitate lentivirus transfection (25). Lentivirus plasmid was constructed by Shanghai Jikai Biotechnology Co., Ltd. (Shanghai, China) (multiplicity of infection=100). Polybrene (Cat#X2351, Inovogen, Carlsbad, CA, USA) at a concentration of 10mg/ml was added to enhance the transfection efficiency. After 12 h, the stable transfection cell line was established by centrifugation. 72 h after transfection, the cells were collected for further treatment.

### Cell groups

Based on distinct treatment protocols, the H9C2 cells were categorized into 4 separate groups: (A): Control group; (B) H/R group: The H9C2 cardiomyocyte model was established by H/R for 5 h (Condition: 1% O<sub>2</sub>, 94% N<sub>2</sub> and 5% CO<sub>2</sub>) and reoxygenation for 1 h (26). (C) Ghrelin overexpression group (Ghrelin): the expression vector of ghrelin was transfected before H/R induction, F: 5'-TGCTCTA-GAATGCCCTCCCCAGGGACCGTCT-3'; R: 5'-CGG GATCCTCACTTGTCGGCTGGGGCCTCTT-3'. (D) Negative control group (NC): Ghrelin empty vector was transfected before H/R induction.

To further study the mechanism of ghrelin alleviating H9C2 myocardial injury induced by H/R, we added compound C, an AMPK inhibitor. In Ghrelin + AMPK inhibitor compound C (Ghrelin+Compound C) group, Ghrelin overexpression vector was transfected before H/R induction, and cells were treated with 5 μM Compound C (Cat#ab120843, Abcam, Cambridge, MA, USA) for 24 h (27).

### RT-PCR

After the H/R model was constructed, the cells of each group were collected. RNA of each group was extracted by TRIzol Kit (Cat#15596-018, Life Technology, Gaithersburg, MD, USA), following the provided instructions. After the RNA concentration was detected, the reverse transcription Kit (Qiagen, Duesseldorf, Germany) was used for reverse transcription. Mastercycler® Nexus X2 (light cycler96, Roche, Basel, Switzerland) was used for qRT-PCR to obtain the cycle threshold of each group. The reaction conditions were as follows: initial denaturation at 94°C for 3 minutes; denaturation at 94°C for 30 seconds, followed by primer annealing at 60°C for 30 seconds, and extension at 72°C for 20 seconds. This cycle was repeated

for 40 times. The 2<sup>-ΔΔCT</sup> method was used for quantitative calculation.

The primer sequence was as follows: Ghrelin Forward: 5'-GGTGTCTTCAGCGACTATCTGC-3'; Reverse: 5'-TCCTCCTCTGCCTCTTCTGC-3'. β-actin Forward: 5'-TGTCACCAACTGGGACGATA-3'; Reverse: 5'-GG-GGTGTTGAAGGTCTCAAA-3'

### CCK8 assay

H9C2 cells in the logarithmic growth phase were enzymatically detached using trypsin and subsequently quantified. Subsequently, the cell concentration was adjusted to 5×10<sup>4</sup> cells/ml and then seeded into a 96-well plate. 100 μl H9C2 cells (5000 cells/well) were added and incubated in 5% CO<sub>2</sub> incubator at 37°C for 12 h (n = 3). Discarding the culture medium, cells were incubated with 10 μl CCK8 (Cat#C0039, Beyotime, Shanghai, China) in 5% CO<sub>2</sub> incubator at 37°C for 4 h. The absorbance (A) of each well was measured at 490 nm wavelength by HBS-1096A microplate reader (Nanjing Detie Experimental Equipment Co., Ltd., Nanjing, China), and the cell survival rate was calculated. Survival rate (%) = (A<sub>experiment</sub> - A<sub>blank</sub>)/(A<sub>control</sub> - A<sub>blank</sub>)×100.

### Flow cytometry

H9C2 cells in the logarithmic growth phase were enzymatically detached using trypsin and subsequently quantified. Subsequently, the cell concentration was adjusted to 2×10<sup>5</sup> cells/ml and then seeded onto a 6-well plate. A volume of 500 μl of H9C2 cells containing 1×10<sup>5</sup> cells per well was introduced into each well and incubated in 5% CO<sub>2</sub> incubator for 12 h at 37°C. Apoptosis was assessed using flow cytometry. The experimental procedure was strictly in accordance with the Annexin V-APC/PI double staining cell apoptosis detection kit (Cat#KA3807, Abnova, Taipei, Taiwan, China). The cells were trypsinized and subsequently centrifuged at 1000 rpm, 4°C for 10 minutes to gather the cellular pellet. Discarded supernatant and added PBS buffer to wash cells twice. The cells were subjected to centrifugation at 1000 rpm, 4°C for 10 minutes. Following the removal of the supernatant, 200 μl 1×binding buffer and 10 μl Annexin V-APC were added to cells. The cells were mixed gently and reacted at room temperature for 15 min. Then 300 μl 1×binding buffer and 5 μl PI were added to cells. The flow cytometry (Gallios; Beckman Coulter, Inc, Brea, California, USA) was used within 1 h (n=3).

### TUNEL

The procedures were meticulously executed in strict accordance with the guidelines provided by the one-step TUNEL cell apoptosis detection kit (Cat#C1090, Beyotime, Shanghai, China). The specific methods are as follows: 0.5 ml H9C2 cells (1×10<sup>6</sup> cells/ml) were cultured on a climbing tablet in 6-well-plate. After the adherent cell growth, 1 ml 4% polyformaldehyde (Cat#P0099, Beyotime, Shanghai, China) were added to each well for 30 min. Then the cells were rinsed once with PBS, added 500 μl 0.3% Triton-X PBS solution and followed by incubation at room temperature for 5 minutes. Following a single wash with PBS, 100 μl TUNEL solution (TdT enzyme 5 μl, Fluorescent marker solution 45 μl and TUNEL test solution) were added to each well. The TUNEL test solution was shaken gently to cover the climbing tablets evenly, and

incubated in dark for 60 min at 37°C. Subsequent to three rounds of washing with PBS, the sealing liquid seal was quenched with anti-fluorescence quenching and observed under BK6000 fluorescence microscope (Chongqing Aote Optical Instrument Co., Ltd., Chongqing, China). Five areas were randomly selected for photo taking, and Image J 1.49p software processing system was used to analyze (n=3). Apoptotic index = (Number of apoptosis-positive cells/Total cell number)×100%

## ELISA

The expression of pro-inflammatory factors secreted by H9C2 cells was detected in accordance with the instructions of ELISA kits (Nanjing Jiancheng Bioengineering Institute, Nanjing, China). H9C2 cells ( $1 \times 10^5$  cells/ml) were inoculated into 24-well-plate, 1 ml/well. After transfection of ghrelin overexpression lentiviral vector, the cells were treated with COV08-0064 for 3 h. The supernatant was collected and stored at -20°C. The expression of TNF- $\alpha$  (H052), IL-6(H007) and IL-1 $\beta$  (H002) were detected by ELISA (n=3).

## Western blotting

The entire protein content was extracted utilizing RIPA lysis buffer (Cat#P0013B, Beyotime, Shanghai, China). The protein concentration was measured by BCA Kit (Cat#PC0020, Solarbio, Beijing, China). 40  $\mu$ g protein was used in 10% SDS-PAGE electrophoretic separation. The electrophoresis time is about 1~1.5 h. Subsequently, the isolated proteins were transferred onto a polyvinylidene fluoride (PVDF) membrane (Cat#XY-f1136, Xinyu Biology). TBST buffer containing 5% skimmed milk powder was sealed at room temperature for 2 h, and the membrane was washed with TBST buffer for 3 times (5 min each time). Added Rabbit anti-rat LC3B (1:1000, ab221794, Abcam, Cambridge, MA, USA), Beclin-1 (1:1000, 3495s, Cell Signaling Technology, Danvers, MA, USA), P62 (1:1000, orb228027, Biorbyt, Cambridge, UK), phospho-AMPK (1:800, ab23875, Abcam, Cambridge, MA, USA), AMPK (1:1000, ab207442, Abcam, Cambridge, MA, USA), phospho-ULK1 (1:900, ab203027, Abcam, Cambridge, MA, USA), ULK1 (1:1000, ab240916, Abcam, Cambridge, MA, USA), phospho-AMBRA1 (Ser52) (1:1000, ABC80, Merck Millipore, Billerica, MA, USA), AMBRA1 (1:800, ab69501, Abcam, Cambridge, MA, USA),  $\beta$ -actin (1:1500, ab8227, Abcam, Cambridge, MA, USA), Incubated overnight at 4°C. Following that, the membranes underwent three wash cycles using TBST (each for 5 minutes). The Goat anti-rabbit IgG H-L (HRP) (1:3000, ab205718, Abcam, Cambridge, MA, USA) was added and incubated at room temperature for 2 h. The membranes were washed 3 times with TBST (5 min each time) and placed in the chemiluminescence reagents (Cat#W028-2-1, Nanjing Institute of Bioengineering, Nanjing, China) for 1 min under the condition of dark. The gel scanning imaging system (K8160, Beijing Ke Chuang Ruixin Biotechnology Co., Ltd., Beijing, China) was used. The grayscale intensity of the bands was quantified using the Image J 1.49p software processing system and made the comparison involved assessing the ratio of each specific target band in relation to the internal reference band (n=3).

## Statistical analyses

Adopted Statistic Package for Social Science (SPSS)

17.0 statistical software (SPSS Inc., Chicago, IL, USA) for analysis. The outcomes of the data analysis were reported as mean  $\pm$  standard deviation (mean  $\pm$  SD). One-way ANOVA was used for data analysis among multiple groups. Tukey test was used in comparison between groups with  $P < 0.05$  as the statistically significant.

## Results

### Effects of ghrelin on the survival and apoptosis of H9C2 cells after H/R injury

As shown in Figures 1A and B, the expression of ghrelin within the H/R group was notably lower compared to the control group ( $P < 0.05$ ). In contrast to the H/R and NC groups, the expression of ghrelin was markedly elevated within the Ghrelin group ( $P < 0.01$ ). The CCK-8 experiment demonstrated that in contrast to the control group, the cell survival rate in both the H/R and NC groups exhibited a remarkable decrease ( $P < 0.01$ ) (Figure 1C). In comparison to the H/R and NC groups, the survival rate of H9C2 cells transfected with the ghrelin lentiviral vector exhibited a remarkable increase ( $P < 0.05$ ) (Figure 1C). As depicted in Figure 1D, following H/R injury, there was a remarkable increase in the apoptosis rate of H9C2 cells when compared to the control group ( $P < 0.01$ ). After transfection of ghrelin vector, the H9C2 cells apoptosis rate decreased significantly ( $P < 0.01$ ), which was remarkably different from that of H/R group and NC group. Consistent with the results of flow cytometry, the TUNEL fluorescence assay revealed a substantial increase in the apoptotic index within the H/R group compared to the control group ( $P < 0.01$ ) (Figure 1E). Compared with H/R group and NC group, the apoptotic index of ghrelin-transfected cells decreased significantly ( $P < 0.01$ ) (Figure 1E).

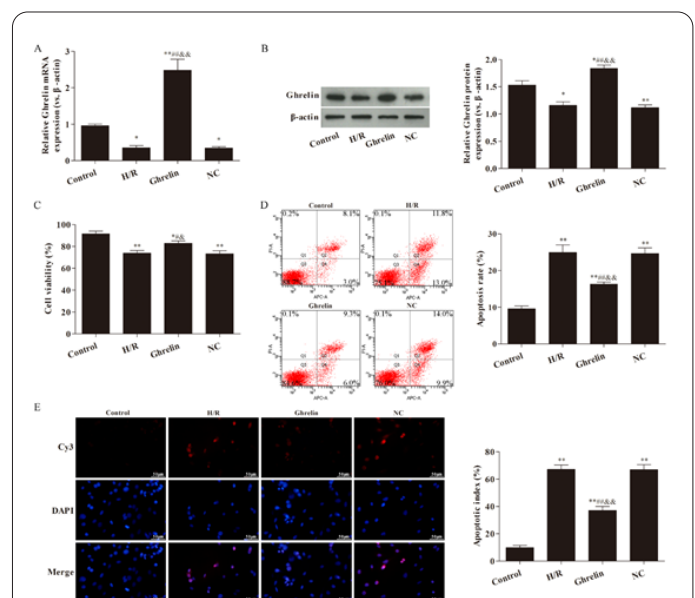


**Figure 1.** The effects of ghrelin on the survival and apoptosis of H9C2 cells after H/R injury. (A and B) The expression of ghrelin was detected by qRT-PCR and WB. (C) CCK8 was used to analyze the effect of ghrelin on the survival rate of H9C2 cells after H/R. (D) The effects of ghrelin on H9C2 cell apoptosis after H/R were analyzed by flow cytometry and TUNEL fluorescence. The magnification is 400 $\times$  (n = 3). Compared with control group, \* $P < 0.05$ , \*\* $P < 0.01$ ; Compared with H/R group, # $P < 0.05$ , ## $P < 0.01$ ; Compared with NC group, & $P < 0.05$ , && $P < 0.01$ .

### Ghrelin inhibits the expression of inflammatory factors in H9C2 cells after H/R injury

As depicted in Figure 2, the concentrations of IL-6, IL-1 $\beta$ , and TNF- $\alpha$  within the H/R group were notably elevated in comparison to the control group ( $P < 0.01$ ). In comparison to the H/R group and NC group, the transfection of the ghrelin vector led to a remarkable downregulation in pro-inflammatory factor expressions ( $P < 0.05$ ).

### Effects of ghrelin on autophagy of H9C2 cells after H/R injury

In comparison to the control group, both the H/R group and the NC group exhibited a remarkable increase in Beclin-1 expression and the ratio of LC3BII/LC3BI, alongside a remarkable decrease in the expression of P62 ( $P < 0.05$ ) (Figure 3). After transfection of ghrelin overexpression vector, Beclin-1 and LC3BII/LC3BI expressions in H/R group and NC group were remarkably increased, while P62 expression was remarkably decreased ( $P < 0.01$ ).

### Effects of ghrelin on AMPK/ULK1 pathway in H9C2 cells after H/R injury

As shown in Figure 4, The phosphorylated forms of AMPK, ULK1 and AMBRA1 were activated in H/R group, and the expressions of p-AMPK, p-ULK1 and p-AMBRA1 were markedly elevated in comparison to the control group ( $P < 0.01$ ). After transfection of ghrelin lentiviral vector into H9C2 cells, the H/R injury model was established, and the expression of the above proteins was

further promoted (Figure 4).

### Ghrelin activates AMPK/ULK1 pathway, promotes cell survival and inhibits apoptosis

As depicted in Figure 5A, the survival rate within the H/R group exhibited a noteworthy increase, while conversely, that of the Ghrelin group experienced a significant decrease ( $P < 0.01$ ) by adding AMPK inhibitor on the basis of ghrelin. As depicted in Figure 5B, the apoptosis rate of H9C2 cells was notably lower compared to the H/R group ( $P < 0.01$ ) and remarkably higher compared to Ghrelin group ( $P < 0.05$ ), this observation aligned with the outcomes obtained from the TUNEL assay (Figure 5C). As

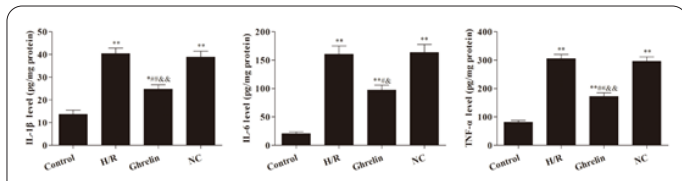


**Figure 2.** The effects of ghrelin on the expression of inflammatory factors in H9C2 cells after H/R injury. The effects of ghrelin on the expression of inflammatory factors (TNF- $\alpha$ , IL-6 and IL-1 $\beta$ ) were analyzed by ELISA (n = 3). Compared with control group, \* $P < 0.05$ , \*\* $P < 0.01$ ; Compared with H/R group, # $P < 0.05$ , ## $P < 0.01$ ; Compared with NC group, & $P < 0.05$ , && $P < 0.01$ .

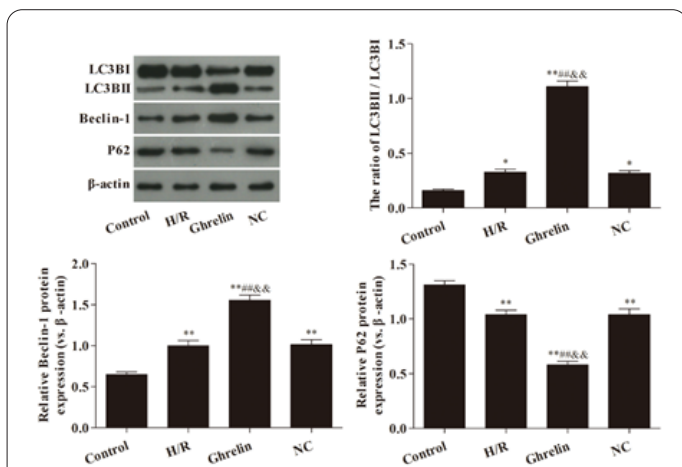


**Figure 3.** The effects of ghrelin on autophagy of H9C2 cells after H/R injury. Western Blotting was used to analyze the effect of ghrelin on the expression of LC3BII/LC3BI, Beclin-1 and P62 of H9C2 cells after H/R injury (n = 3). Compared with control group, \* $P < 0.05$ , \*\* $P < 0.01$ ; Compared with H/R group, # $P < 0.05$ , ## $P < 0.01$ ; Compared with NC group, & $P < 0.05$ , && $P < 0.01$ .

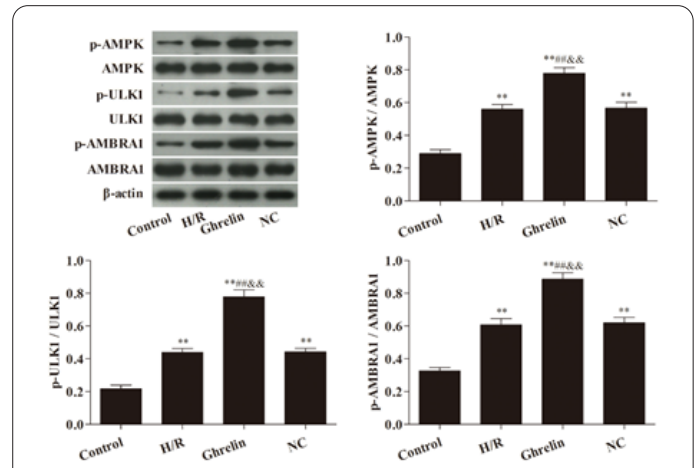


**Figure 4.** Effects of ghrelin on AMPK/ULK1 pathway in H9C2 cells after H/R injury. Western Blotting was used to analyze the effect of ghrelin on the expression of p-AMPK, AMPK, p-ULK1, ULK1, p-AMBRA1 and AMBRA1 in AMPK/ULK1 pathway of H9C2 cells after H/R injury (n = 3). Compared with control group, \* $P < 0.05$ , \*\* $P < 0.01$ ; Compared with H/R group, # $P < 0.05$ , ## $P < 0.01$ ; Compared with NC group, & $P < 0.05$ , && $P < 0.01$ .

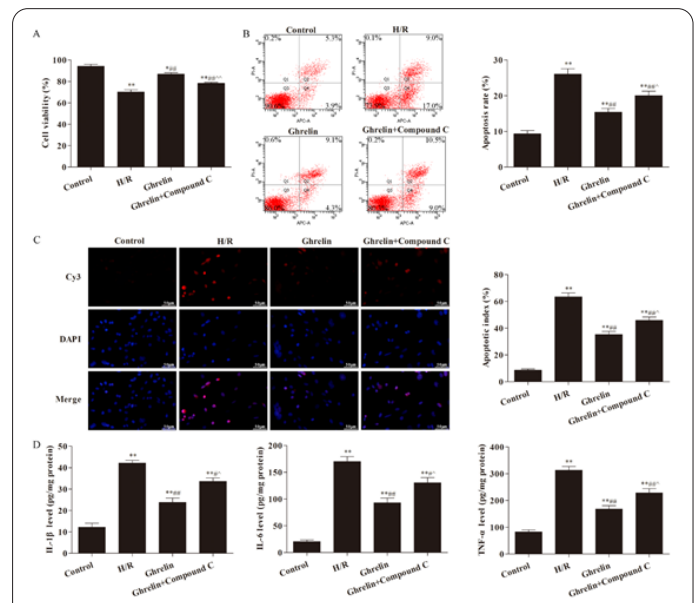


**Figure 5.** Ghrelin activated AMPK/ULK1 pathway, promoted cell survival and inhibited apoptosis. (A) CCK8 assay was used to detect cell survival. (B and C) flow cytometry and TUNEL fluorescence were used to analyze cell apoptosis. The magnification is 400 $\times$ . (D) ELISA kit were used to detect the expressions of IL-1 $\beta$ , IL-6 and TNF- $\alpha$  cells. Compared with control group, \* $P < 0.05$ , \*\* $P < 0.01$ ; Compared with H/R group, # $P < 0.05$ , ## $P < 0.01$ ; Compared with Ghrelin group, ^ $P < 0.05$ , ^^ $P < 0.01$ .

shown in Figure 5D, ghrelin inhibited the inflammatory response induced by H/R, while IL-6, IL-1 $\beta$  and TNF- $\alpha$  levels were remarkably higher than that in ghrelin group when given ghrelin and Compound C in the same time ( $P < 0.05$ ).

### Ghrelin promotes autophagy by activating AMPK/ULK1 pathway

As depicted in Figure 6, when compared to the ghrelin group, LC3BII/LC3BI and Beclin-1 expression levels within the Ghrelin+Compound C group exhibited a notable decrease. Conversely, P62 expression was remarkably increased ( $P < 0.05$ ).

### Ghrelin activates AMPK/ULK1 pathway

As depicted in Figure 7, p-AMPK, p-ULK1, and p-AMBRA1 expressions were markedly elevated within the Ghrelin group when compared to the H/R group ( $P < 0.01$ ). After being given ghrelin and compound C, the expressions of the above proteins were inhibited, which was remarkably different from those of the Ghrelin group ( $P < 0.05$ ).

### Discussion

In our study, H9C2 cells were transfected with ghrelin overexpression lentiviral vector and the hypoxia/reoxygenation H9C2 model was constructed. Previous studies have shown that ghrelin can stimulate growth hormone secretion, and regulate appetite and metabolism (28). Ghrelin also plays a protective role in some cardiovascular diseases (29). Nonetheless, the precise cellular and molecular mechanisms underlying the cardioprotective effects of ghrelin remain incompletely understood. Previous studies have proved that ghrelin can reduce oxidative damage of the stomach, brain, blood vessels and liver (30-32). In this study, we found that H/R injury decreased ghrelin expression. Ghrelin overexpression can significantly promote cell survival, reduce apoptosis, activate AMPK, ULK1 and AMBRA1, promote autophagy, increase LC3BII and Beclin-1 expressions, and reduce P62 expression and inflammatory response.

Previous studies have shown that ghrelin can induce autophagy in neurons and hepatocytes by activating AMPK (33). AMPK serves as a vital intracellular energy sensor (34). The AMPK/ULK1 signaling pathway is capable of initiating autophagy in response to oxidative stress and inflammation (35). In this study, we found that ghrelin overexpression was up-regulated during ghrelin-induced autophagy in H9C2 cells. In addition, the inactivation of AMPK inhibited this activity. Our data indicates that ghrelin has the capability to trigger autophagy, increase LC3BII/LC3BI and Beclin-1 expression, and decrease P62 expression. Inhibition of AMPK resulted in the enhancement of these proteins-induced effects. Furthermore, we delved into the mechanism by which AMPK, ULK1, and AMBR1 regulate the autophagy induced by ghrelin. The relationship between AMPK and autophagy has been documented in prior research studies. For example, AMPK regulates autophagy through deacetylation of mTOR, ATG and FoxO1 proteins and the SIRT1/AMPK signaling pathway (36).

ATG proteins hold significant importance in the autophagic process. The deacetylation of ATG7, ATG5, and

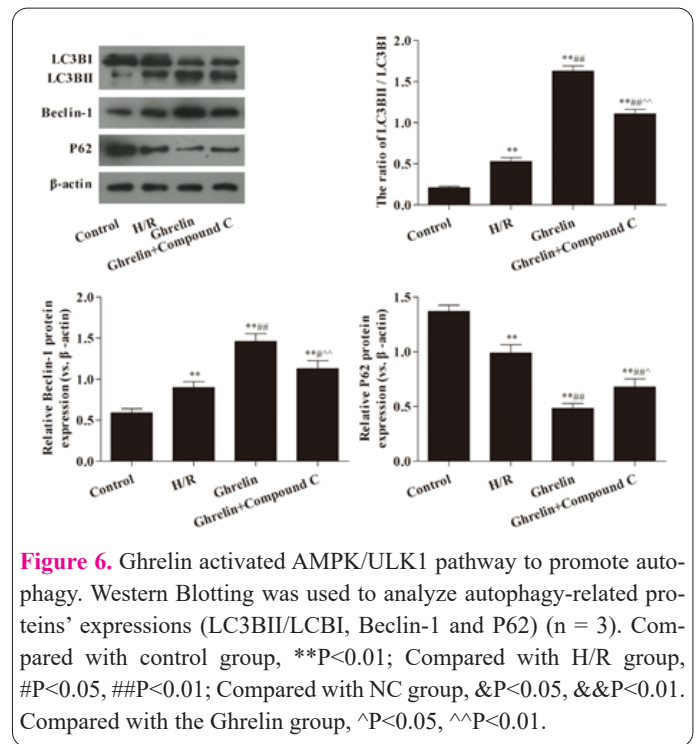


**Figure 6.** Ghrelin activated AMPK/ULK1 pathway to promote autophagy. Western Blotting was used to analyze autophagy-related proteins' expressions (LC3BII/LC3BI, Beclin-1 and P62) ( $n = 3$ ). Compared with control group,  $**P < 0.01$ ; Compared with H/R group,  $\#P < 0.05$ ,  $\#\#P < 0.01$ ; Compared with NC group,  $\&P < 0.05$ ,  $\&\&P < 0.01$ . Compared with the Ghrelin group,  $\wedge P < 0.05$ ,  $\wedge\wedge P < 0.01$ .

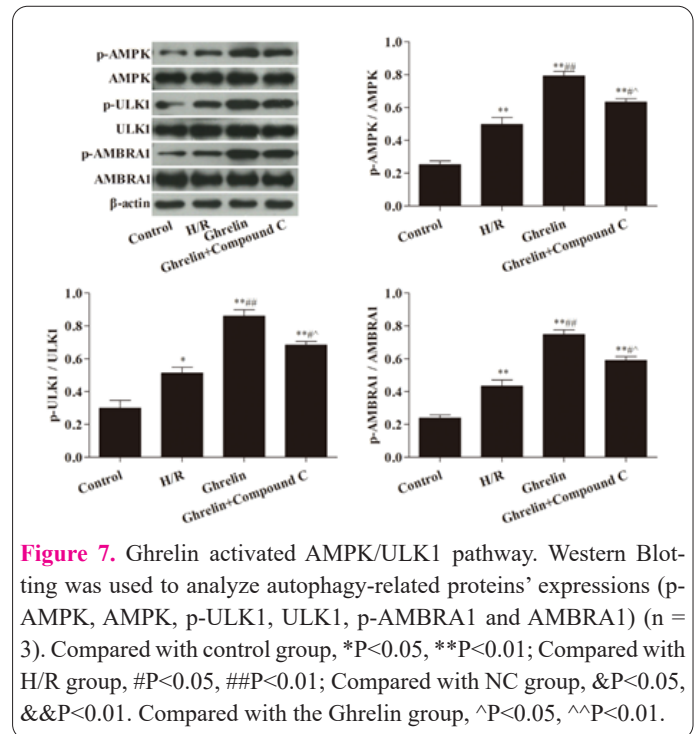


**Figure 7.** Ghrelin activated AMPK/ULK1 pathway. Western Blotting was used to analyze autophagy-related proteins' expressions (p-AMPK, AMPK, p-ULK1, ULK1, p-AMBRA1 and AMBRA1) ( $n = 3$ ). Compared with control group,  $*P < 0.05$ ,  $**P < 0.01$ ; Compared with H/R group,  $\#P < 0.05$ ,  $\#\#P < 0.01$ ; Compared with NC group,  $\&P < 0.05$ ,  $\&\&P < 0.01$ . Compared with the Ghrelin group,  $\wedge P < 0.05$ ,  $\wedge\wedge P < 0.01$ .

LC3 (ATG8) facilitated by AMPK is crucial for triggering autophagy in response to starvation (37). ATG5 and Beclin-1 (yeast ATG6 homolog) are two autophagy-related proteins essential for autophagy formation. They not only promote autophagy formation but also induce apoptosis (16). They are considered as molecular switch proteins regulating autophagy and apoptosis. P62 (SQSTM 1 protein) can play the role of autophagy and apoptosis in tumor cells. P62 consists of four domains: PB1, TB, LIR and UBA. The LIR domain is responsible for binding to ATG8/LC3 (38). Hence, we hypothesize that the AMPK/ULK1 pathway might be involved in ghrelin-induced autophagy via the deacetylation of LC3. In this study, we found ghrelin activated the AMPK/ULK1 pathway and enhanced autophagy.

Our experiments confirm that ghrelin can inhibit H9C2

cardiomyocyte apoptosis and inflammatory response induced by hypoxia/reoxygenation, activating AMPK/ULK1 pathway and autophagy.

### Disclosure statement

All authors declared that there was no conflict of interest.

### Abbreviation

AMPK, Adenosine 5'-monophosphate (AMP)-activated protein kinase; ULK1, unc-51 like autophagy activating kinase 1; AMBRA1, autophagy and beclin 1 regulator 1; LC3B, light chain 3 beta; P62, sequestosome 1; qRT-PCR, Quantitative Real-time PCR; CCK8, Cell Counting Kit-8; TUNEL, TdT-mediated dUTP nick end labeling; ELISA, Enzyme-linked immunosorbent assay.

### Acknowledgements

None.

### Statement of Ethics

None

### Funding

None.

### Availability of data and materials

Please contact the authors for data requests.

### References

- Lin TC, Hsiao M. Ghrelin and cancer progression. *Bba-Rev Cancer* 2017; 1868(1): 51-57.
- Beiras-Fernandez A, Kreth S, Weis F, et al. Altered myocardial expression of ghrelin and its receptor (GHSR-1a) in patients with severe heart failure. *Peptides* 2010; 31(12): 2222-2228.
- Broglio F, Gottero C, Prodam F, et al. Non-acylated ghrelin counteracts the metabolic but not the neuroendocrine response to acylated ghrelin in humans. *J Clin Endocr Metab* 2004; 89(6): 3062-3065.
- Gauna C, Delhanty PJ, Hofland LJ, et al. Ghrelin stimulates, whereas des-octanoyl ghrelin inhibits, glucose output by primary hepatocytes. *J Clin Endocr Metab* 2005; 90(2): 1055-1060.
- Hattori N. Expression, regulation and biological actions of growth hormone (GH) and ghrelin in the immune system. *Growth Horm Igf Res* 2009; 19(3): 187-197.
- Duxbury MS, Waseem T, Ito H, et al. Ghrelin promotes pancreatic adenocarcinoma cellular proliferation and invasiveness. *Biochem Bioph Res Co* 2003; 309(2): 464-468.
- Oz M, Dikel S. Effect of garlic (*Allium sativum*)-supplemented diet on growth performance, body composition and fatty acid profile of rainbow trout (*Oncorhynchus mykiss*). *Cell Mol Biol* 2022; 68(1): 217-225.
- Mizushima N. Autophagy: process and function. *Gene Dev* 2007; 21(22): 2861-2873.
- Nakatogawa H, Ichimura Y, Ohsumi Y. Atg8, a ubiquitin-like protein required for autophagosome formation, mediates membrane tethering and hemifusion. *Cell* 2007; 130(1): 165-178.
- Pankiv S, Alemu EA, Brech A, et al. FYCO1 is a Rab7 effector that binds to LC3 and PI3P to mediate microtubule plus end-directed vesicle transport. *J Cell Biol* 2010; 188(2): 253-269.
- Bouchelaghem R, Mader S, Gaboury L, Messarah M, Boumendjel M, Boumendjel A. Estrogens desensitize MCF-7 breast cancer cells to apelin-induced autophagy and enhanced growth under estrogen starvation: a possible implication in endocrine resistance. *Cell Mol Biol* 2022; 68(9): 113-124.
- Komatsu M, Kageyama S, Ichimura Y. p62/SQSTM1/A170: physiology and pathology. *Pharmacol Res* 2012; 66(6): 457-462.
- Huang R, Xu Y, Wan W, et al. Deacetylation of nuclear LC3 drives autophagy initiation under starvation. *Mol Cell* 2015; 57(3): 456-466.
- Komatsu M, Waguri S, Koike M, et al. Homeostatic levels of p62 control cytoplasmic inclusion body formation in autophagy-deficient mice. *Cell* 2007; 131(6): 1149-1163.
- Li X, Wang Y, Xiong Y, et al. Galangin Induces Autophagy via Deacetylation of LC3 by SIRT1 in HepG2 Cells. *Sci Rep-Uk* 2016; 6: 30496.
- Sui X, Chen R, Wang Z, et al. Autophagy and chemotherapy resistance: a promising therapeutic target for cancer treatment. *Cell Death Dis* 2013; 4(10): e838.
- Hariharan N, Maejima Y, Nakae J, Paik J, Depinho RA, Sadoshima J. Deacetylation of FoxO by Sirt1 Plays an Essential Role in Mediating Starvation-Induced Autophagy in Cardiac Myocytes. *Circ Res* 2010; 107(12): 1470-1482.
- Hardie DG. AMP-activated/SNF1 protein kinases: conserved guardians of cellular energy. *Nat Rev Mol Cell Bio* 2007; 8(10): 774-785.
- Canto C, Gerhart-Hines Z, Feige JN, et al. AMPK regulates energy expenditure by modulating NAD<sup>+</sup> metabolism and SIRT1 activity. *Nature* 2009; 458(7241): 1056-1060.
- Kim J, Kundu M, Viollet B, Guan KL. AMPK and mTOR regulate autophagy through direct phosphorylation of Ulk1. *Nat Cell Biol* 2011; 13(2): 132-141.
- Han X, Tai H, Wang X, et al. AMPK activation protects cells from oxidative stress-induced senescence via autophagic flux restoration and intracellular NAD(+) elevation. *Aging Cell* 2016; 15(3): 416-427.
- Jin X, Chen M, Yi L, et al. Delphinidin-3-glucoside protects human umbilical vein endothelial cells against oxidized low-density lipoprotein-induced injury by autophagy upregulation via the AMPK/SIRT1 signaling pathway. *Mol Nutr Food Res* 2014; 58(10): 1941-1951.
- Talero E, Alcaide A, Avila-Roman J, Garcia-Maurino S, Vendramini-Costa D, Motilva V. Expression patterns of sirtuin 1-AMPK-autophagy pathway in chronic colitis and inflammation-associated colon neoplasia in IL-10-deficient mice. *Int Immunopharmacol* 2016; 35: 248-256.
- White E. Deconvoluting the context-dependent role for autophagy in cancer. *Nat Rev Cancer* 2012; 12(6): 401-410.
- Feng X, Luo Q, Wang H, Zhang H, Chen F. MicroRNA-22 suppresses cell proliferation, migration and invasion in oral squamous cell carcinoma by targeting NLRP3. *J Cell Physiol* 2018; 233(9): 6705-6713.
- Benoist L, Chadet S, Genet T, et al. Stimulation of P2Y11 receptor protects human cardiomyocytes against Hypoxia/Reoxygenation injury and involves PKCepsilon signaling pathway. *Sci Rep-Uk* 2019; 9(1): 11613.
- Hong SH, Hwang HJ, Kim JW, et al. Ginsenoside compound-Mc1 attenuates oxidative stress and apoptosis in cardiomyocytes through an AMP-activated protein kinase-dependent mechanism. *J Ginseng Res* 2020; 44(4): 664-671.
- Rodriguez A, Gomez-Ambrosi J, Catalan V, et al. The ghrelin O-acyltransferase-ghrelin system reduces TNF-alpha-induced apoptosis and autophagy in human visceral adipocytes. *Diabetologia* 2012; 55(11): 3038-3050.
- Mao Y, Wang J, Yu F, et al. Ghrelin reduces liver impairment in a model of concanavalin A-induced acute hepatitis in mice. *Drug Des Devel Ther* 2015; 9: 5385-5396.
- Ezquerro S, Mendez-Gimenez L, Becerril S, et al. Acylated and

- desacyl ghrelin are associated with hepatic lipogenesis, beta-oxidation and autophagy: role in NAFLD amelioration after sleeve gastrectomy in obese rats. *Sci Rep-Uk* 2016; 6: 39942.
31. Ezquerro S, Mocha F, Fruhbeck G, et al. Ghrelin Reduces TNF-alpha-Induced Human Hepatocyte Apoptosis, Autophagy, and Pyroptosis: Role in Obesity-Associated NAFLD. *J Clin Endocr Metab* 2019; 104(1): 21-37.
  32. Mao Y, Cheng J, Yu F, Li H, Guo C, Fan X. Ghrelin Attenuated Lipotoxicity via Autophagy Induction and Nuclear Factor-kappaB Inhibition. *Cell Physiol Biochem* 2015; 37(2): 563-576.
  33. Okatsu K, Saisho K, Shimanuki M, et al. p62/SQSTM1 cooperates with Parkin for perinuclear clustering of depolarized mitochondria. *Genes Cells* 2010; 15(8): 887-900.
  34. Kundu M, Lindsten T, Yang CY, et al. Ulk1 plays a critical role in the autophagic clearance of mitochondria and ribosomes during reticulocyte maturation. *Blood* 2008; 112(4): 1493-1502.
  35. Strappazon F, Nazio F, Corrado M, et al. AMBRA1 is able to induce mitophagy via LC3 binding, regardless of PARKIN and p62/SQSTM1. *Cell Death Differ* 2015; 22(3): 419-432.
  36. Nazio F, Strappazon F, Antonioli M, et al. mTOR inhibits autophagy by controlling ULK1 ubiquitylation, self-association and function through AMBRA1 and TRAF6. *Nat Cell Biol* 2013; 15(4): 406-416.
  37. White E, Mehnert JM, Chan CS. Autophagy, Metabolism, and Cancer. *Clin Cancer Res* 2015; 21(22): 5037-5046.
  38. Wu Y, Li X, Zhu JX, et al. Resveratrol-activated AMPK/SIRT1/autophagy in cellular models of Parkinson's disease. *Neurosignals* 2011; 19(3): 163-174.